

See discussions, stats, and author profiles for this publication at: <https://www.researchgate.net/publication/253948702>

# Preparation of poly( $\gamma$ -benzyl-L-glutamate) nanofibers by electrospinning from isotropic and biphasic liquid crystal solutions

ARTICLE in POLYMER JOURNAL · JANUARY 2012

Impact Factor: 1.65 · DOI: 10.1038/pj.2011.137

CITATIONS

3

READS

54

## 8 AUTHORS, INCLUDING:



**Kazuma Tsuboi**

Tokyo Institute of Technology

35 PUBLICATIONS 280 CITATIONS

SEE PROFILE



**Minoru Ashizawa**

Tokyo Institute of Technology

36 PUBLICATIONS 238 CITATIONS

SEE PROFILE



**Hidemine Furuya**

Tokyo Institute of Technology

84 PUBLICATIONS 981 CITATIONS

SEE PROFILE



**Akihiko Tanioka**

Tokyo Institute of Technology

203 PUBLICATIONS 2,916 CITATIONS

SEE PROFILE

## ORIGINAL ARTICLE

# Preparation of poly( $\gamma$ -benzyl-L-glutamate) nanofibers by electrospinning from isotropic and biphasic liquid crystal solutions

Kazuma Tsuboi<sup>1</sup>, Erika Marcelletti<sup>2</sup>, Hidetoshi Matsumoto<sup>1</sup>, Minoru Ashizawa<sup>1</sup>, Mie Minagawa<sup>1</sup>, Hidemine Furuya<sup>1</sup>, Akihiko Tanioka<sup>1</sup> and Akihiro Abe<sup>3</sup>

Liquid crystal polymer (LCP) nanofibers were prepared by electrospinning from isotropic and biphasic poly( $\gamma$ -benzyl-L-glutamate) (PBLG)/dichloromethane–pyridine solutions. The prepared fibers were characterized by scanning electron microscopy, Fourier-transform infrared spectroscopy, polarized optical microscopy, wide-angle X-ray diffraction and polarized micro-Raman spectroscopy. The as-spun PBLG fiber from the isotropic solutions had an undulating orientation of closed-packed  $\alpha$ -helices similar to a serpentine trajectory in their internal structures. The as-spun PBLG fibers from the biphasic solutions that contained the LC phase had uniaxially oriented hexagonal lattices of  $\alpha$ -helices along the fiber axis. These results indicated that the orientation of the ordered structure of the electrospun lyotropic LCP fibers can be controlled by the initial microstructure of the spinning solution.

*Polymer Journal* (2012) 44, 360–365; doi:10.1038/pj.2011.137; published online 11 January 2012

**Keywords:** electrospinning; lyotropic liquid crystal polymer; nanofiber; poly( $\gamma$ -benzyl-L-glutamate)

## INTRODUCTION

Electrospinning is a straightforward and versatile method for the formation of continuous thin fibers that is based on an electrohydrodynamic process. This method has the advantages of (i) being applicable for a broad spectrum of molecules, such as inorganic molecules, synthetic polymers, proteins and DNA and (ii) the ability to produce thin fibers with diameters in the micrometer and nanometer ranges.<sup>1–4</sup> Electrospun fibers, or fibrous fabrics with high surface areas, have recently attracted much attention for their applications in high-performance filter media, protective clothing, battery separator and electrode materials, drug delivery systems and biomaterial scaffolds for tissue engineering.<sup>1–4</sup> Many properties of the nanofibers, such as the mechanical, electrical and optical properties, depend not only on the intrinsic properties of the polymer but also on the internal structure of the fibers. Therefore, control of the internal structure and molecular orientation of the nanofibers is required for improvement of their properties. Recently, some researchers have reported that electrospinning is a useful process for controlling the crystal morphology and molecular orientation of poly(ethylene oxide),<sup>5</sup> polyoxymethylene<sup>6</sup> and poly(vinylidene fluoride) nanofibers.<sup>7</sup> In addition, we have reported that the formation and orientation of the ordered structure in the electrospun liquid crystalline polymer (LCP) fibers could be controlled by the fiber diameter during electrospinning of the main-chain liquid crystalline (LC) polyester, BB-5(3-Me), solutions.<sup>8</sup>

Poly( $\gamma$ -benzyl-L-glutamate) (PBLG, see Figure 1) is a synthetic polypeptide that adopts a rigid rod-like  $\alpha$ -helical conformation ( $\alpha$ -helix) in organic solvents.<sup>9</sup> In general, the  $\alpha$ -helices in a polypeptide show a lyotropic LC characteristic that forms a chiral nematic phase or hexagonal columnar LC phase in concentrated solutions and condensed materials.<sup>9–13</sup> Because the  $\alpha$ -helix possesses a large dipole moment (3.4 Debye per peptide), the polar ordered structure of PBLG is a candidate for soft materials with macro-dipole moments for applications in pyroelectric and piezoelectric devices as well as electro-optic devices. To obtain polar ordering of the  $\alpha$ -helices in solution or film of PBLG, external fields, such as a flow field, magnetic field or electric field, have been used.<sup>14–16</sup> Therefore, during electrospinning, the  $\alpha$ -helices are expected to be highly oriented in an electrified thin solution jet. Ohkawa *et al.* have reported the preparation of PBLG nanofibers by electrospinning from various PBLG solutions. They revealed that the electrospinning process changes the chain conformation from a random coil to an  $\alpha$ -helix and that the  $\alpha$ -helical conformation in the spinning solution leads to a higher crystallinity in the as-spun fibers.<sup>17</sup> More recently, Yu *et al.* have reported that electrospun PBLG microfibers ( $\sim 4\ \mu\text{m}$ ) have a permanent polarity and piezoelectricity.<sup>18</sup> However, studies on the effect of the ordered structures of the spinning solution on the internal structure and molecular orientation of electrospun PBLG nanofibers have not yet been conducted.

<sup>1</sup>Department of Organic and Polymeric Materials, Tokyo Institute of Technology, Meguro-ku, Japan; <sup>2</sup>Faculty of Mechanical Engineering, RWTH Aachen University, Aachen, Germany and <sup>3</sup>Professor Emeritus, Tokyo Institute of Technology, Tokyo, Japan

Correspondence: Dr A Tanioka, Department of Organic and Polymeric Materials, Tokyo Institute of Technology, Ookayama, Meguro-ku, Tokyo 152-8552, Japan.

E-mail: tanioka.a.aa@m.titech.ac.jp

Received 10 August 2011; revised 9 November 2011; accepted 14 November 2011; published online 11 January 2012

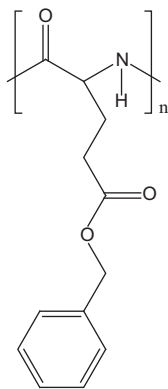


**Figure 1** Chemical structure of PBLG.

In the present study, we focused on the preparation of PBLG fibers with highly oriented ordered structures by electrospinning from the biphasic solution (that is, mixture of isotropic and lyotropic LC phases).<sup>10–12,19</sup> A solution in the complete LC phase of PBLG in which  $\alpha$ -helices are highly oriented and aggregated is difficult to electrospin because of its high viscosity. The biphasic of lyotropic LC appears between the intermediate concentration between critical concentrations for the isotropic and LC phase at a certain temperature,<sup>10–12,19</sup> and the biphasic solution can be electrospun. The aims of the present study were (i) to prepare PBLG nanofibers by electrospinning from both isotropic and biphasic solutions and (ii) to investigate the effect of the ordered structure in the spinning solution (that is, the ordered structure in the biphasic solution) on the internal structure and molecular orientation of the electrospun fibers. The prepared fibers were characterized by scanning electron microscopy (SEM), Fourier-transform infrared spectroscopy, polarized optical microscopy (POM), wide-angle X-ray diffraction (WAXD) and polarized micro-Raman spectroscopy.

## EXPERIMENTAL PROCEDURE

### Materials

PBLG ( $M_w$ =231 300) and dichloromethane ( $\text{CH}_2\text{Cl}_2$ ) of extra-pure grade were purchased from Sigma-Aldrich Japan (Tokyo, Japan). Pyridine of extra-pure grade was purchased from Wako (Osaka, Japan). All reagents were used without further purification. PBLG was dissolved in  $\text{CH}_2\text{Cl}_2$  at concentrations of 7.5 and 8 wt%, which are near the critical concentration between the isotropic phase and biphasic phase (mixture of the isotropic and LC phases) that is known as ‘point A’.<sup>12,19</sup> Pyridine was added to the solvent at a concentration of 1.0 weight percent to improve the electrospinnability. Figure 2 shows the POM images of the PBLG/ $\text{CH}_2\text{Cl}_2$ -pyridine solutions. The 7.5 wt% solution exhibited an isotropic phase, whereas the 8 wt% solution exhibited a biphasic structure (mixture of the LC phase and isotropic phase based on the texture of the spherulites).<sup>19</sup>

### Electrospinning

The electrospinning setup was the same as that previously described.<sup>20</sup> The electrospinning device consisted of a syringe-type infusion pump (MCIP-III, Minato Concept, Tokyo, Japan) and a high-voltage regulated DC power supply (HAR-100P0.3, Matsusada Precision, Kusatsu, Japan). We used a rotating disk as a collector to align the electrospun fibers (disk diameter: 250 mm, width: 3 mm). The polymer solutions were contained in a syringe with a stainless steel nozzle (0.57 mm inner diameter). For electrospinning, the fiber diameter depends on the solution properties (for example, viscosity, conductivity, surface tension, permittivity and boiling point) and/or operating conditions (for example, applied voltage, nozzle-to-collector distance and flow rate).<sup>2,3</sup> In

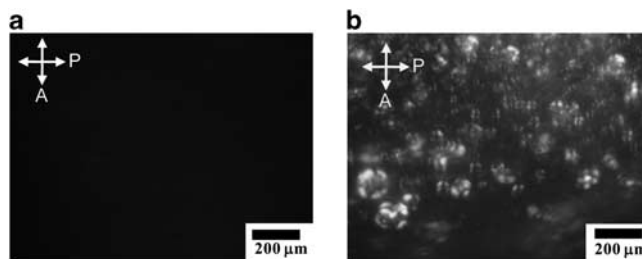


**Figure 2** Polarized micrographs of the PBLG solution at concentrations of (a) 7.5 wt% and (b) 8.0 wt%, in  $\text{CH}_2\text{Cl}_2$  containing 1 wt% pyridine. A full color version of this figure is available at *Polymer Journal* online.

particular, the applied voltage and the flow rate are crucial factors for controlling the fiber diameter.<sup>20–22</sup> In the present study, the applied voltage for the spinning and flow rate of the solution were set at 11.0–39.5 kV and 0.1–0.5  $\text{ml min}^{-1}$ , respectively. The nozzle-to-collector distance was fixed at 10 or 12 cm, and the rotating speed of the collector was 500 r.p.m. The spinning conditions are summarized in Table 1. All spinnings were performed under room temperature at  $24 \pm 1.5^\circ\text{C}$  and 30–50% relative humidity.

### Characterization

The morphologies of the prepared PBLG fibers were observed using a SEM (SM-200, Topcon, Tokyo, Japan) operated at 10 kV. All samples were sputter-coated with Au. The infrared spectra of the prepared fibers were measured using the attenuated total reflectance method using a Fourier-transform infrared spectrometer (FTIR-4200, JASCO, Tokyo, Japan) with 48 scans at a resolution of  $4\text{ cm}^{-1}$ . The fiber samples were set on a germanium attenuated total reflectance prism. POM observations were conducted using a polarized microscope (BX-51, Olympus, Tokyo, Japan) in transmittance geometry with crossed polarizers. The  $\times 100$  objective lens (NA 0.98) was used for microscopic observation of the fibers. For observation of the orientation of the LC directors in the fibers, the fiber axis was rotated  $45^\circ$  in a counter-clockwise direction from the polarization direction and set parallel to the polarization axis. WAXD patterns of the prepared uniaxially aligned fibers were measured by irradiation using monochromatic Cu K $\alpha$  radiation generated by an X-ray generator (UltraX18, Rigaku, Tokyo, Japan) and recorded on an imaging plate. The axial direction of the aligned fiber samples was set along the equator direction of the imaging plate. The polarized micro-Raman spectra of the prepared uniaxially aligned fibers were measured using a 3D Raman microscopy system (Nano-finder 30, Tokyo Instruments, Tokyo, Japan). As a light source, 514.5-nm radiation from an argon-ion laser (Innova300, COHERENT, Santa Clara, CA, USA) was used. The irradiated power of the excitation beam was  $\sim 20\text{ mW}$  at the sample surface. The beam was focused with a  $\times 20$  lens (NA 0.40) on the surface of the aligned fibers. The polarization of the beam was controlled by a half-wave plate. The polarized Raman spectra were obtained by averaging the signals of three measurements accumulated in 100 s.

## RESULTS AND DISCUSSION

Figure 3 shows typical SEM images of the as-spun PBLG fibers from the isotropic PBLG solution (7.5 wt%). We succeeded in preparing homogeneous (bead-free) fibers with diameters from 1.67 to 0.65  $\mu\text{m}$  by electrospinning from the isotropic solution at various applied voltages and flow rates. Figure 4 shows a typical Fourier-transform infrared spectroscopy spectrum for the electrospun PBLG fibers from the isotropic solution. In the spectrum, the characteristic peaks of the  $\alpha$ -helical conformation in a peptide, amide II ( $1542\text{ cm}^{-1}$ ), amide I ( $1650\text{ cm}^{-1}$ ) and C=O stretch ( $1731\text{ cm}^{-1}$ ) were clearly observed. The peak position of the amide I indicates a right-handed  $\alpha$ -helical conformation of PBLG in the fibers ( $1650\text{--}1655\text{ cm}^{-1}$ ).<sup>23,24</sup> Figure 5 shows the POM images of the as-spun PBLG fibers from the isotropic solution deposited on a glass slide with crossed polarizers in which the polarization of the incident light was horizontal in the figures. In

**Table 1** Spinning conditions of PBLG/CH<sub>2</sub>Cl<sub>2</sub>-pyridine solutions

Solution	Applied voltage (kV)	Distance (cm)	Flow rate (ml min <sup>-1</sup> )	Mean fiber diameter (mm)	Fiber alignment
Isotropic <sup>a</sup>	11	10	300	1.67 ± 0.29	Random
	11	12	200	1.35 ± 0.509	Aligned <sup>b</sup>
	27.5	12	100	0.95 ± 0.23	Random
	39.5	12	500	1.43 ± 0.19	Random
	39.5	10	300	1.11 ± 0.17	Random
	39.5	12	100	0.83 ± 0.30	Random
	39.5	10	100	0.65 ± 0.22	Aligned <sup>b</sup>
Biphasic <sup>a</sup>	39.5	10	100	0.65 ± 0.15	Aligned <sup>b</sup>

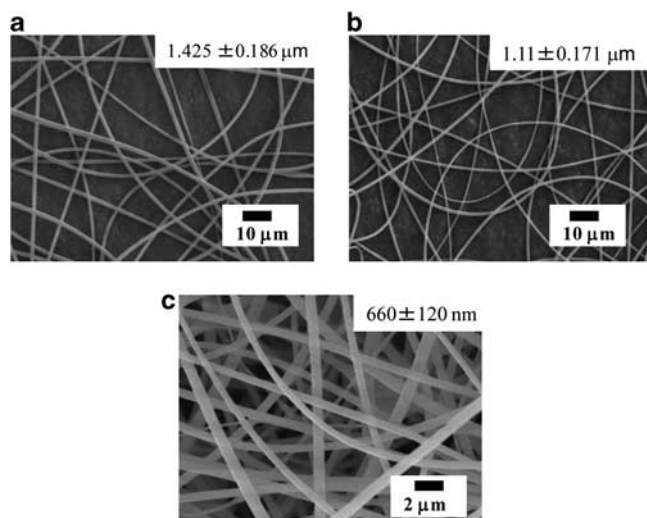
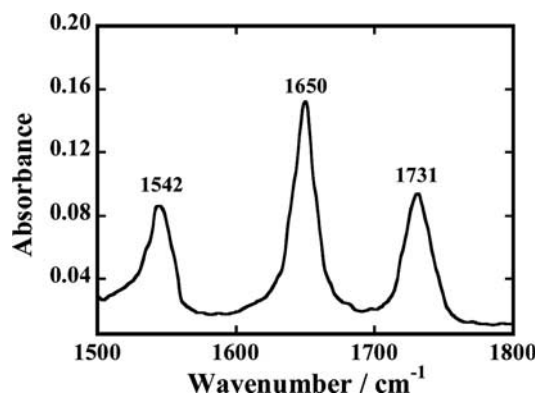
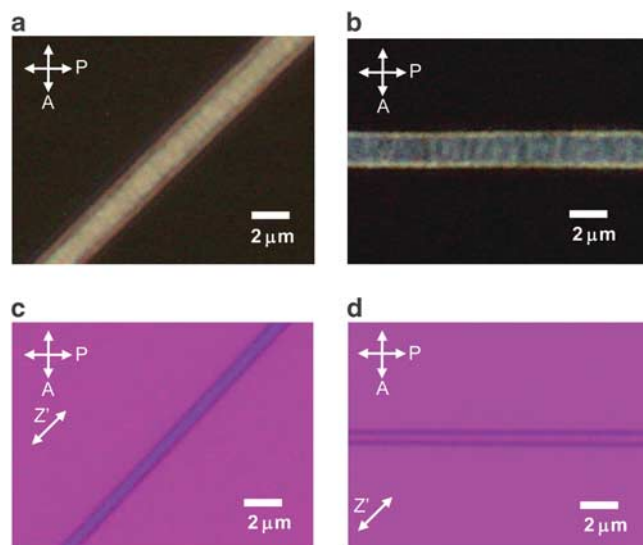
<sup>a</sup>The compositions of the isotropic and biphasic PBLG solutions were PBLG/CH<sub>2</sub>Cl<sub>2</sub>/pyridine = 7.5/91.6/0.9 and 8/91.1/0.9 in weight ratio, respectively.<sup>b</sup>Fiber alignment on the collector was controlled by a rotating disk.**Figure 3** SEM images of PBLG fibers electrospun from isotropic solution at an applied voltage of 39.5 kV. The diameter was controlled by the flow rate of the 7.5 wt% CH<sub>2</sub>Cl<sub>2</sub> (pyridine 1.0 wt%) solution: (a) 500 μl min<sup>-1</sup>, (b) 300 μl min<sup>-1</sup> and (c) 100 μl min<sup>-1</sup>.**Figure 4** Fourier-transform infrared spectroscopy spectrum of the 0.65-μm-thick PBLG nanofibers prepared from isotropic solution.

Figure 5a, both the birefringence along the fiber axis and the periodical striations across the fiber axis in the PBLG fiber with a diameter ( $D$ ) of 2 μm are observed, and the periodicity scale of the striations is ~0.6–0.7 μm. Figure 5b, in which the polarization of light is parallel to the fiber axis, also shows the striations in the fiber. These periodical

**Figure 5** POM images of the 2-μm-diameter PBLG fiber prepared from isotropic solution (a) for LC directors along the fiber axis and (b) for directors oblique to the fiber axis. The images of the 0.72-μm-diameter PBLG fiber (c) for LC directors along the fiber axis and (d) for LC directors oblique to the fiber axis. Arrows in the inset show the directions of polarization (P) and the analyzer (A). For observation of (c) and (d), a sensitive color plate was inserted; the Z-direction of the sensitive color plate is indicated by the oblique arrow.

striations in the POM observation of PBLG are known as a ‘banded texture’, which is commonly observed for PBLG and other LCPs after the cessation of elongation or shearing because of orientation relaxation processes<sup>25,26,27</sup> and one of the hexagonal columnar textures.<sup>13</sup> The appearance of the banded texture is understood to be an undulation of the molecular orientation of LCP, such as a serpentine trajectory because of orientation relaxation, in which the period of the striation corresponds to the half period of the serpentine trajectory (that is, the period of the trajectory is 1.2–1.4 μm).<sup>13</sup> However, in the POM image of the PBLG fiber with a  $D$  value of 0.72 μm, no banded texture was observed with the crossed polarizers (Figures 5c and d), whereas birefringence along the fiber axis was clearly observed (Figure 5c). This result suggests that improvement orientation of  $\alpha$ -helices occurs from serpentine orientation to uniaxial orientation along the fiber axis. We measured the birefringence along the fiber axis,  $\Delta n$ , which reflects the average orientation of the LC director, for the fibers with various diameters deposited on the glass substrate using the Senarmont’s method. In Figure 6, the obtained  $\Delta n$  was plotted as a

function of the fiber diameter. As the fiber diameter decreased,  $\Delta n$  increased to a maximum of  $\sim 0.091$  at  $0.66\ \mu\text{m}$ . This result also suggests that the molecular orientation of PBLG is improved with thinning of the fiber diameter toward a uniaxial orientation from the undulated molecular orientation.

According to a study of the PBLG orientation under shear by Larson and Mead, the LC directors, whose average orientation is parallel to the shearing direction, readily vary toward a uniaxial orientation along the shearing direction compared with the directors with a random orientation.<sup>26</sup> Herein, we examined the effect of the ordered LC structure of the spinning solution on the internal structure of the fibers using isotropic and biphasic PBLG/ $\text{CH}_2\text{Cl}_2$ -pyridine solutions (the concentrations of the isotropic and biphasic solutions were 7.5 wt% and 8 wt%, respectively).<sup>27,28</sup> We prepared nanofibers from the isotropic and biphasic solutions based on the conditions

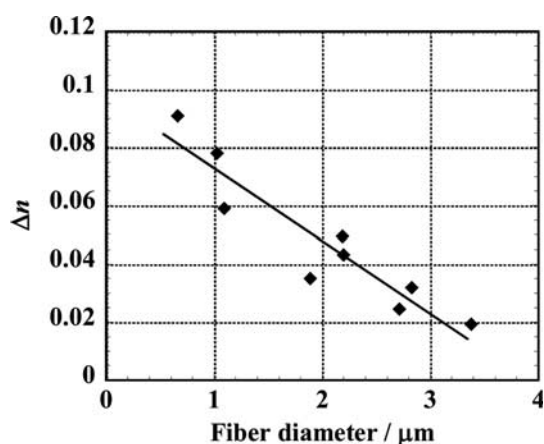


**Figure 6** The dependence of the birefringence  $\Delta n$  on the fiber diameter in PBLG fibers electrospun from isotropic solution obtained using the Senarmont's method. The value of  $\Delta n$  was obtained from samples prepared from isotropic solutions under the conditions listed in Table 1.

listed in Table 1. As previously mentioned, the birefringence measurement showed that the internal orientation of the PBLG depends on the fiber diameter. In this study, we fixed the fiber diameter at the thinnest value ( $D=0.65\ \mu\text{m}$ ) for purposes of comparison. The Fourier-transform infrared spectroscopy spectra of both nanofibers exhibited a right-handed  $\alpha$ -helical conformation of PBLG, and the spectra were identical to the spectrum shown in Figure 4. Polarized microscopic observations of the nanofibers did not show a banded structure in the fibers. We do not employ the  $\Delta n$  obtained from the nanofibers to discuss the molecular orientation in the nanofibers because the birefringence obtained from nanofibers includes errors because of their diameter being smaller than the resolution limit of an objective lens,  $\delta \sim 1.22\lambda / \text{NA} \sim 0.685\ \mu\text{m}$  at  $\lambda \sim 550\ \text{nm}$ . Figure 7 shows the SEM images and WAXD patterns for the aligned PBLG nanofibers electrospun from the isotropic and biphasic solutions. In both WAXD patterns, diffraction peaks that correspond to separations of 5.25 and  $13.3\ \text{\AA}$  were observed. These separations are attributed to the hexagonal lattice of the closed-packed structure of the rod-like  $\alpha$ -helices:<sup>11,18</sup> the former separation is the longitudinal periodicity of the  $\alpha$ -helices, and the latter one is similar to the reported transversal lattice constant of the hexagonal closed-packed structure of the  $\alpha$ -helices.<sup>9,11,29,30</sup> The WAXD pattern for the nanofiber from the isotropic solution ( $D=0.65\ \mu\text{m}$ , Figure 7b) exhibited peaks slightly concentrated on the pole and the equator, which suggests a uniaxial orientation of a small fraction of the hexagonal lattice, whereas the pattern for the thicker aligned fiber electrospun from the isotropic solution ( $D=1.35\ \mu\text{m}$ ) exhibited Debye-Scherrer rings (Supplementary Figure S1). This improvement in the orientation is consistent with the fiber-diameter dependence of  $\Delta n$ . In contrast, the pattern for the nanofiber from the biphasic solution clearly showed a uniaxial orientation of the hexagonal lattice parallel to the fiber axis (Figure 7d). The orientational order parameter of the closed-packed hexagonal lattices for the nanofiber from the biphasic solution was determined to be  $S=1/2$  ( $3 < \cos^2\beta > -1$ )  $\sim 0.45$  from azimuth profiles of both the diffraction peaks in the WAXD pattern (Supplementary Figure S2).<sup>31</sup> In addition, the orientation of the  $\alpha$ -helices in the nanofibers was investigated by

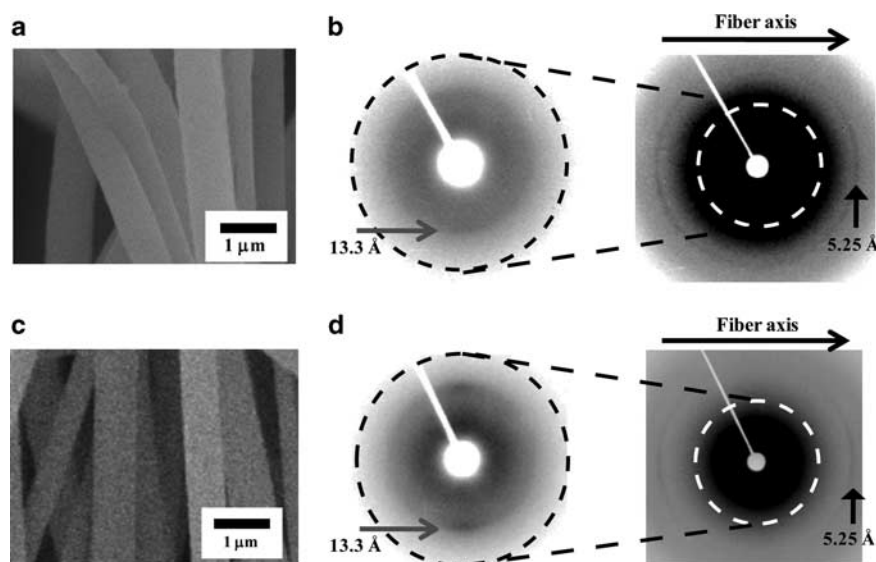


**Figure 7** SEM images and WAXD patterns of aligned electrospun PBLG nanofibers; (a) SEM image and (b) WAXD pattern of the nanofibers from isotropic solution and (c) the image and (d) the pattern of the nanofibers from biphasic solution. In the WAXD patterns, the fiber axis corresponds to the equator direction.



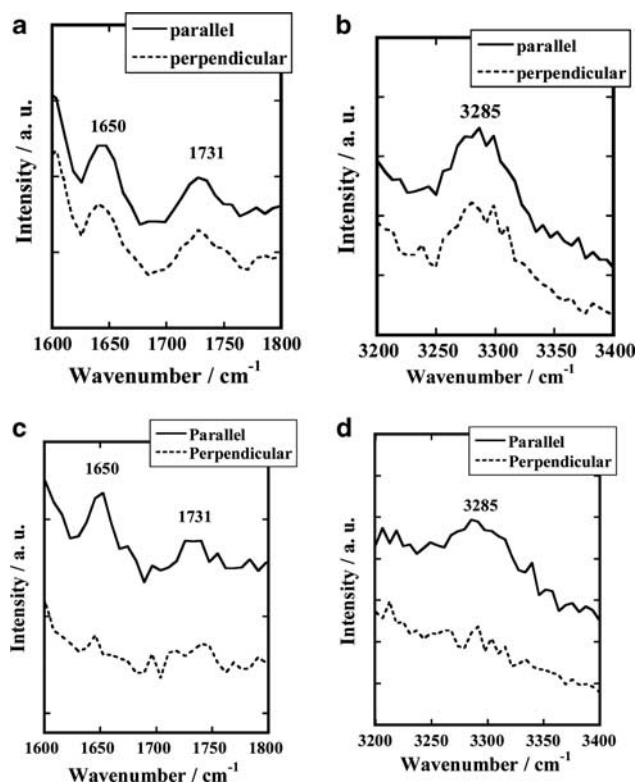


**Figure 8** Polarized micro-Raman spectra of aligned PBLG nanofibers; panels (a) and (b) depict the spectra of aligned PBLG nanofibers prepared from isotropic solution; panels (c) and (d) depict the spectra of the fibers from biphasic solution. The mean fiber diameters were both 0.65  $\mu\text{m}$ .

polarized micro-Raman spectroscopy using the bands of amide I ( $1650\text{ cm}^{-1}$ ) and N-H stretching ( $3285\text{ cm}^{-1}$ ), which are allowed only with the polarization parallel to the principal axis of the  $\alpha$ -helix.<sup>32</sup> For the nanofibers from the isotropic solution, the polarized micro-Raman spectrum is independent of the polarization (Figures 8a and b), which indicates the low orientation order parameter of the  $\alpha$ -helices. For the PBLG nanofibers spun from the biphasic solution, the bands of amide I and N-H stretching were observed only with the polarization parallel to the fiber axis (Figures 8c and d). This result suggests a uniaxial orientation of the  $\alpha$ -helices along the fiber axis in the nanofiber from the biphasic solution. Both the WAXD and polarized micro-Raman spectroscopy showed low-orientational-order orientations and uniaxial orientations of the hexagonal lattices in the nanofibers prepared from the isotropic solution and the biphasic solution, respectively. The orientational order parameter cannot be obtained from polarized micro-Raman spectroscopy because of the low signal-to-noise ratio. Based on these results, we concluded that the fibers from the isotropic solution include a significant amount of the undulating orientational structure of the hexagonal lattice, like a serpentine trajectory, as shown in Figure 9a. In contrast, the nanofiber from the biphasic solution exhibits uniaxial orientation of the hexagonal lattices (Figure 9b). The nanofiber from the isotropic solution includes a small fraction of latter orientational structure, as evidenced by the WAXD pattern (see Figure 7a and Supplementary Figure S2), whereas the undulating orientational structure is the primary orientational structure. For electrospinning from the isotropic solution, rapid solidification due to solvent evaporation prevents the formation of the highly ordered internal

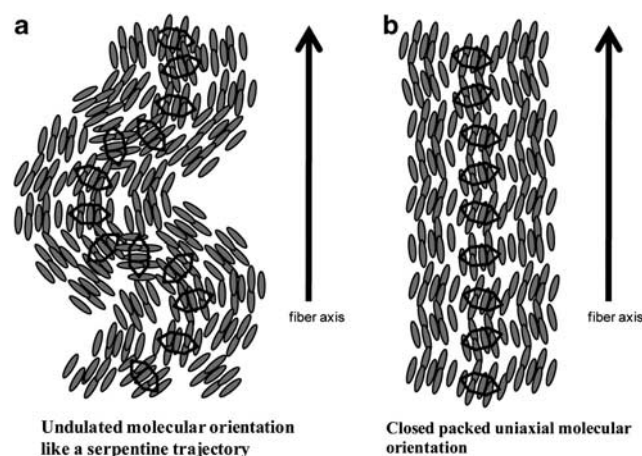


**Figure 9** Proposed internal molecular orientational structures for PBLG fibers. (a) Undulated molecular orientation for the fibers from isotropic solution and (b) closed-packed uniaxial molecular orientation for the nanofiber from biphasic solution. Ellipses show mesogens of PBLG. The hexagon depicted by a solid line indicates the hexagonal lattice of the closed-packed structure of the  $\alpha$ -helix coils. Random coil parts of the segment between the coils were abbreviated.

structure of the  $\alpha$ -helices.<sup>31</sup> Thus, the resulting nanofibers would be non-homogeneous in density and easily distorted by the orientation relaxation process, such as buckling of the jet on the collector, which leads to the undulated orientational structure of the hexagonal lattices. However, the uniaxial orientation of PBLG would be formed by electrospinning from the biphasic solution as follows. First, the LC mesophases of PBLG in the biphasic solution are oriented by the extrusion process of the viscous solution through the spinneret nozzle.<sup>31,32</sup> These previously oriented LC mesophases could serve as templates for the uniaxial orientation of the other  $\alpha$ -helices.<sup>28</sup> Therefore, the successive electrostatic extension of the electrified liquid jet along its axis readily orients the  $\alpha$ -helices parallel to the flow direction of the liquid jet despite the rapid solidification of the liquid jet.<sup>21,27,28,33</sup> In addition, the highly ordered structure homogeneously formed in the jet would not be significantly distorted by the orientational relaxation processes. These findings revealed that the orientation of the ordered structure in the electrospun PBLG nanofiber is controlled by the initial microstructure of the spinning solutions.

## CONCLUSION

In the present study, LCP nanofibers were prepared by electrospinning from isotropic and biphasic PBLG/ $\text{CH}_2\text{Cl}_2$ -pyridine solutions. The as-spun PBLG fibers from the isotropic solutions had a serpentine trajectory molecular orientation of the  $\alpha$ -helices in their internal structures. The as-spun PBLG fibers from the biphasic solutions that contained the LC phase had a uniaxially oriented closed-packed structure of the  $\alpha$ -helices in their internal structures. These results indicated that the orientation of the ordered structure of the electrospun lyotropic LCP fibers can be controlled by the microstructure of the spinning solution. In particular, electrospinning from the LCP solutions that contain the LC phase is a promising option for the preparation of LCP nanofibers with highly oriented and ordered structures. More detailed investigations of the relationship between the ordered structures of LCP solutions and the internal structure of electrospun LCP will enable us to more precisely control the formation and orientation of the ordered structure of the electrospun LCP fibers. The electrospun PBLG fibers that contain highly oriented  $\alpha$ -helices

will be promising materials for application not only in pyroelectric and piezoelectric devices, but also in electro-optic devices.

## ACKNOWLEDGEMENTS

We thank Professor Hideo Takezoe, Associate Professor Masatoshi Tokita and Dr Tsuyoshi Michinobu, Tokyo Institute of Technology, for assistance with the polarized micro-Raman spectroscopy, WAXD and FT-IR/ATR measurements, respectively. This study was partly supported by the New Energy and Industrial Technology Department Organization (NEDO).

- 1 Doshi, J. & Reneker, D. H. Electrospinning process and applications of electrospun fibers. *J. Electrostatics* **35**, 151–160 (1995).
- 2 Reneker, D. H. & Chun, I. Nanometre diameter fibres of polymer, produced by electrospinning. *Nanotechnology* **7**, 216–223 (1996).
- 3 Li, D. & Xia, Y. Electrospinning of nanofibers: reinventing the wheel? *Adv. Mater.* **16**, 1151–1170 (2004).
- 4 Greiner, A. & Wendorff, J. H. Electrospinning: a fascinating method for the preparation of ultrathin fibers. *Angew. Chem. Int. Ed.* **46**, 5670–5703 (2007).
- 5 Kakade, M. V., Givens, S., Gardner, K., Lee, K. H., Chase, D. B. & Rabolt, J. F. Electric field induced orientation of polymer chains in macroscopically aligned electrospun polymer nanofibers. *J. Am. Chem. Soc.* **129**, 2777–2782 (2007).
- 6 Kongkhlang, T., Tashiro, K., Kotaki, M. & Chirachanchai, S. Electrospinning as a new technique to control the crystal morphology and molecular orientation of polyoxymethylene nanofibers. *J. Am. Chem. Soc.* **130**, 15460–15466 (2008).
- 7 Danno, T., Matsumoto, H., Nasir, M., Shimizu, S., Minagawa, M., Kawaguchi, J., Horibe, H. & Tanioka, A. Fine structure of PVDF nanofiber fabricated by electrospray deposition. *J. Polym. Sci. B: Polym. Phys.* **46**, 58–563 (2008).
- 8 Nakashima, K., Tsuboi, K., Matsumoto, H., Ishige, R., Tokita, M., Watanabe, J. & Tanioka, A. Control over internal structure of liquid crystal polymer nanofibers by electrospinning. *Macromol. Rapid Commun.* **31**, 1641–1645 (2010).
- 9 Pauling, L. & Corey, R. B. Two hydrogen-bonded spiral configurations of the polypeptide chain. *J. Am. Chem. Soc.* **72**, 5349 (1950).
- 10 Robinson, C. Liquid-crystalline structures in solutions of a polypeptide. *Trans. Faraday Soc.*, **52**, 571–592 (1956).
- 11 Robinson, C. Liquid-crystalline structures in solutions of a polypeptide. Part 2. *Trans. Faraday Soc.* **25**, 29–42 (1958).
- 12 Flory, P. J. Phase changes in proteins and polypeptides. *J. Polymer Sci.* **49**, 105–128 (1961).
- 13 Livolant, F. & Bouligan, Y. Liquid crystalline phases given by helical biological polymers (DNA, PBLG and xanthan). Columnar textures. *J. Physique* **47**, 1813–1827 (1986).
- 14 Panar, M. & Phillips, W. D. Magnetic ordering of poly- $\gamma$ -benzyl-L-glutamate solutions. *J. Am. Chem. Soc.* **90**, 3880–3882 (1968).
- 15 Orwoll, R. D. & Vold, R. L. Molecular order in liquid crystalline solutions of poly( $\gamma$ -benzyl L-glutamate) in dichloromethane. *J. Am. Chem. Soc.* **93**, 5335–5338 (1971).
- 16 Yen, C., Taguchi, Y., Tokita, M. & Watanabe, J. Spontaneous formation of polar liquid crystal in lyotropic solution of helical poly( $\alpha$ -benzyl glutamate). *Mol. Cryst. Liq. Cryst.* **516**, 91–98 (2010).
- 17 Minato, K., Ohkawa, K. & Yamamoto, H. Chain conformations of poly( $\gamma$ -benzyl-L-glutamate) pre and post an electrospinning process. *Macromol. Biosci.* **6**, 487–495 (2006).
- 18 Farrar, D., Ren, K., Cheng, D., Kim, S., Moon, W., Wilson, W. L., West, J. E. & Yu, S. M. Permanent polarity and piezoelectricity of electrospun  $\alpha$ -helical poly( $\alpha$ -amino acid) fibers. *Adv. Mat.* **23**, 3954–3958 (2011).
- 19 Sakamoto, R. Phase separation of poly( $\gamma$ -benzyl L-glutamine) to liquid crystal and isotropic solution in various helicogenic solvents. *Colloid & Polymer Sci.* **232**, 788–792 (1984).
- 20 Imaizumi, S., Matsumoto, H., Konosu, Y., Tsuboi, K., Minagawa, M., Tanioka, A., Koziol, K. & Windle, A. Top-down process based on electrospinning, twisting, and heating for producing one-dimensional carbon nanotube assembly. *ACS Appl. Mater. Interfaces* **3**, 469–475 (2011).
- 21 Thompson, C. J., Chase, G. G., Yarin, A. L. & Reneker, D. H. Effects of parameters on nanofiber diameter determined from electrospinning model. *Polymer* **48**, 6913–6922 (2007).
- 22 Nasir, M., Matsumoto, H., Danno, T., Minagawa, M., Irisawa, T., Shiota, M. & Tanioka, A. Control of diameter, morphology, and structure of PVDF nanofiber fabricated by electrospray deposition. *J. Polym. Sci. B: Polym. Phys.* **44**, 779–786 (2006).
- 23 Lee, N. H., Christensen, L. M. & Frank, C. W. Morphology of Vapor-Deposited Poly( $\alpha$ -amino acid) Films. *Langmuir* **19**, 3525–3530 (2003).
- 24 Venyaminov, S. Y. & Kalnin, N. N. Quantitative IR spectrophotometry of peptide compounds in water (H<sub>2</sub>O) solutions. II. Amide absorption bands of polypeptides and fibrous proteins in  $\alpha$ -,  $\beta$ -, and random coil conformations. *Biopolymers* **30**, 1259–1271 (1990).
- 25 Viney, C., Donald, A. M., & Windle, A. H. Optical microscopy of banded structures in oriented thermotropic polymers. *J. Mat. Sci.* **18**, 1136–1142 (1983).
- 26 Larson, R. G. & Mead, D. W. Development of orientation and texture during shearing of liquid-crystalline polymers. *Liquid Crystals* **12**, 751–768 (1992).
- 27 Malkin, A. Y., Semakov, A. V. & Kulichikhin, V. G. Self-organization in the flow of complex fluids (colloid and polymer systems) Part 1: Experimental evidence. *Adv. Colloid Interface Sci.* **157**, 75–90 (2010).
- 28 Walker, L. M., Kernick III, W. A. & Wagner, N. J. *In situ* analysis of the defect texture in liquid crystal polymer solutions under shear. *Macromolecules* **30**, 508–514 (1997).
- 29 Corstjens, T., Rastogi, S. & Lemstra, P. A Study on the ordering of intercalated solvents in poly-benzyl-L-glutamate; *in-situ* Raman and X-ray scattering investigations. *Macromol. Symp.* **138**, 105–110 (1999).
- 30 Yamane, Y., Kanekiyo, M., Koizumi, S., Zhao, C., Kuroki, S. & Ando, I. Preparation and characterization of highly oriented poly( $\gamma$ -benzyl L-glutamate) networks and gels with long channels with micrometer-scale diameters. *J. Appl. Polym. Sci.* **92**, 1053–1060 (2004).
- 31 Davidson, J. A., Junga, H. T., Hudson, S. D. & Percec, S. Investigation of molecular orientation in melt-spun high acrylonitrile fibers. *Polymer* **41**, 3357–3364 (2000).
- 32 Tsuboi, M., Ueda, T. & Ushizawa, K. Localized Raman tensors in some biopolymers. *J. Mol. Struct.* **352/353**, 509–517 (1995).
- 33 Ma, M., Krikorian, V., Yu, J. H., Thomas, E. L. & Rutledge, G. C. Electrospun polymer nanofibers with internal periodic structure obtained by microphase separation of cylindrically confined block copolymers. *NanoLett.* **6**, 2969–2972 (2006).

Supplementary Information accompanies the paper on Polymer Journal website (<http://www.nature.com/pj>)